PCCP

Accepted Manuscript

ROYAL SOCIETY OF CHEMISTRY

www.rsc.org/pccp

Insights into gas-phase reaction mechanisms of small carbon radicals using isomer-resolved product detection

Adam J. Trevitt[1]* *and Fabien Goulay*[2]*

[1] School of Chemistry, University of Wollongong, Wollongong, NSW, 2522, Australia

[2] Department of Chemistry, West Virginia University, Morgantown, West Virginia 26506, USA

*adamt@uow.edu.au

*Fabien.goulay@mail.wvu.edu

ABSTRACT

For reactive gas-phase environments, including combustion, extraterrestrials atmospheres and our Earth's atmosphere, the availability of quality chemical data is essential for predictive chemical models. These data include reaction rate coefficients and product branching fractions. This perspective overviews recent isomer-resolved production detection experiments for reactions of two of the most reactive gas phase radicals, the CN and CH radicals, with a suite of small hydrocarbons. A particular focus is given to flow-tube experiments using synchrotron photoionization mass spectrometry. Coupled with computational studies and other experiment techniques, flow tube isomer-resolved product detection have provided significant mechanistic details of these radical + neutral reactions with some general patterns emerging.

Brief Biography

Adam J. Trevitt is an Associate Professor in the School of Chemistry at the University of Wollongong, Australia. He earned his PhD at the University of Melbourne with Prof. Evan Bieske and continued as a postdoc at UC Berkeley and LBNL in the group of Prof. Stephen Leone. Trevitt's research group is working to better understand radical chemistry affecting combustion, atmospheric chemistry and biological processes while also investigating ion spectroscopy and single microdroplet systems.

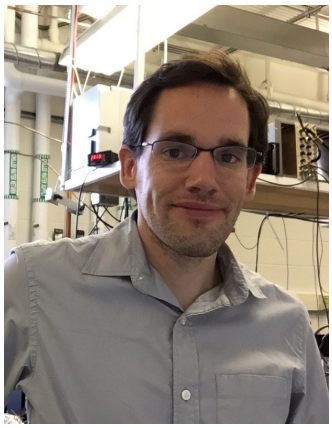

Fabien Goulay is an Assistant Professor in the Department of Chemistry at West Virginia University in Morgantown, WV. He received his PhD from the University of Rennes (France) under the direction of Dr. Bertrand Rowe and continued as a postdoctoral fellow in the group of Prof. Stephen Leone at UC Berkeley and with Dr. Hope A. Michelsen at Sandia National Laboratories. Goulay's research focuses on the understanding of combustion radical processes in the gas phase and at the surface of nanoparticles.

1. Introduction

For reactive gas-phase environments, the availability of quality chemical data is essential to ensure the construction of useful chemical models. Models of combustion, atmospheric chemistry, extraterrestrial atmospheres and the interstellar medium – covering an extensive range of temperature and pressure conditions – require reaction rate coefficients and product branching fractions to ensure they can track and predict evolving chemical populations. These sorts of models target, for example, the evolution of NO_x species in combustion,[1-3] the formation of aromatics on Titan[4-7] or the growth of secondary aerosols in our atmosphere.[8,9] The ongoing testing and refinement of these models has, in turn, driven major advancements in the understanding of fundamental gas-phase radical chemistry and compelled the development of new experimental techniques.

The focus of this Perspective article is the gas-phase reactions of CH and CN radicals with a range of hydrocarbon reactants with emphasis on recent, isomer-specific, product-detection studies and mechanistic insights. Both radicals are known as key species in the gas-phase chemistry in extraterrestrial environments in particular the atmosphere of Titan – where their formation is attributed to many photolysis, electron-attachment and ion-molecule reactions.[6] The reaction of these radicals are thus incorporated into models to predict the molecular composition of the Titanian atmosphere,[10] aerosol/haze[7] and lakes[11]. Both radicals are key players in combustion chemistry with the CH radical widely used as a diagnostic of flame chemistry and dynamics.[12] Both CN and CH radicals are well suited for detection by laser-induced fluorescence (LIF). Fitting their rotationally-resolved LIF spectra provides flame temperature.[13]

Gas-phase kinetics measurements for reactions of small radicals like CN and CH have been conducted over a broad range of temperatures including extremely low temperatures ~13 K and high temperatures up to 1200 K.[14-18] Shock tube experiments can extend to further extremes (<8000 K, <1000 bar).[19,20] The crossed molecular-beams (CMB) technique, in tandem with computational thermodynamics

and RRKM calculations, has delivered major insights into the reaction dynamics of such radical species with hydrocarbons.[21-23] Recently, the coupling of flow reactors commonly used in kinetics experiments to VUV photoionization mass spectrometry has provided product branching fractions of radical reactions with isomer specific detail.[21,24-26] Together with kinetics, reaction dynamics and isomer specific product branching ratios, our understanding of radical-neutral chemistry continues to advance at a rapid pace.

2. Isomer-resolved product detection

The experimental requirements for isomer-resolved product detection are both qualitative and quantitative. It is desirable to identify the presence of all product isomers and determine the branching ratio of the corresponding product pathway(s). Of course, multiple pathways can lead to the same product isomer. A detection method that distinguishes between isomers should, ideally, be applicable to a large range of product species. At the same time, the method should provide quantitative detail – at least relatively – for establishing product branching fractions and thus providing insight into the reaction mechanism. As we will show below, synchrotron photoionization mass spectrometry does, for many reactive chemical systems, satisfy these requirements.

Mass spectrometry coupled to electron impact or photoionization is a common technique employed to detect reaction products in CMB experiments as well as in slow and fast flow reactor experiments.[21] The energy of the ionizing electrons or photons can be either fixed or tuned over an energy range to cover the product ionization thresholds. Kaiser and coworkers[27-31] have used 80 eV electron impact to detect reaction products under single collision conditions. In this case the isomeric information about the mass-selected products are inferred from the translational energy and angular distribution of the products coupled to isotopic labeling of the initial reactants. Under similar conditions, Casavecchia and coworkers[32] have used tunable electron impact ionization (7-100 eV, with 700 meV energy resolution) in order to characterize the products both by their angle distribution and electron ionization energy. One significant advantage is to be able to ionize weakly bound species such as the acetyl radical without fragmentation of the cations.[32]

Soft photo-ionization presents the same advantages as soft electron-impact ionization but with enhanced energy resolution. In this context, "soft" means that the photoionization is not concomitant with significant amounts of cation dissociation. By tuning UV photons just over the molecular ionization thresholds, cation dissociation is minimized and thus the mass spectrometry is not additionally complicated by dissociation product ions. Single-photon laser ionization has been used in CMB to detect H-atom products.[33] In fast flow reactors, Loison et al.[34] have identified the OH + propene reaction products and stabilized adducts by examining ion fragmentation patterns subsequent to laser ionization at 10.54 eV.

Tuning the energy of the ionizing radiation close to the ionization threshold allows for product identification on the basis of mass-to-charge ratio (*m/z*) and ionization energy. With sufficient resolution, isomers and enantiomers – should they have different ionization energy – may be distinguished when formed by the same chemical reaction. Although tunable VUV laser radiation is obtainable through resonance-enhanced wave mixing[35] it has not been extensively employed for studying radical chemistry due to the tunability range limitations. Synchrotron VUV sources, however, are generally tunable over extensive photon energy ranges with very high photon densities, which increases sensitivity. Within the last two decades, synchrotron radiation sources have been coupled to CMB,[36-38] various pyrolysis sources, reactors and flames.[25,39-43]

The Advanced Light Source (LBNL, USA) 1.9 GeV synchrotron is equipped with an undulator-based VUV beamline that provides photons ranging from ~ 7.0 eV up to 14 eV with an energy resolution of ~ 5 - 25 meV.[26,40] This energy range covers ionization thresholds for a vast number of organic molecules and radical species. For detecting isomer products from a gaseous source, photoion mass spectra are recorded while stepping the energy of the incident photons. For each mass channel a photoionization spectrum is recorded by tracking the ion signal as a function of photon energy. When the mass spectrometer is a time-of-flight arrangement a large portion of *m/z* values are detected with good duty factors. The advantage of this multiplex mass spectrometric detection is to collect the photoionization spectra of most of the

chemical species in a single measurement. Species within the gas-mixture are then determined by noting ionization onsets and/or the shape of the photoionization spectra. Kinetic profiles for detected species also assist with their assignment. When the ions are time-tagged on detection, secondary chemistry can be identified.[44] Comparing measured spectra to reference absolute ionization cross-sections for each individual isomer can ultimately provide product branching ratios.

An extension to the synchrotron photoionization mass spectrometry technique is imaging photoelectron-photoion coincidence (iPEPICO) spectroscopy.[42,45] It is fair to say that the technique generally offers cleaner differentiation between isomers as the threshold photoelectron spectra of organic cations usually display sharp vibronic peaks signifying the presence of particular isomers. A good example of this was the recent study of xylyl radical pyrolysis.[46] The article by Bodi et al. discusses the virtues of the iPEPICO method for isomer-specific detection of gas-phase mixtures.[45]

Laboratory-based tabletop techniques continue to develop for the isomer-specific product detection of gas-phase species. Near-infrared femtosecond laser pulse can be used to selectively ionize isomers through strong field ionization.[47,48] The laser dependence of the ion signal as well as the fragmentation patterns can be used to identify isomers from complex mixtures. Recent experiments have also demonstrated the ability of chirped-pulse millimeter-wave spectroscopy to identify radicals and closed shell molecules in pyrolysis environments.[49-51] After expansion cooling to temperatures down the 4 K, this technique allows selective detection of isomers as well as enantiomers using pure rotational spectroscopy.

Isomer-resolved branching ratios are available both from CMB and flow tube experiments. One must be very careful when directly comparing data from these two techniques as they are typically performed over very different energy ranges and under different collisional conditions. In the case of flow tubes, the significant buffer-gas collision rate ($>10^6$ s^{-1}) requires consideration as the increased gas number density may lead to further chemistry/isomerisation. Under single collision conditions of the CMB experiment, the detected products are unequivocally formed by collision of the studied reactants. Because of these large

differences in experimental conditions, both techniques are complementary. Flow tube techniques provide information about temperature and pressure effects (for combustion and atmospheric environments) while CMB methods provide more fundamental information about the fate of reaction intermediates under collision-free conditions.

But, as yet, there is no "panacea" experiment for the universal, quantitative isomer-specific detection of complex gas-phase products. Furthermore, it is typical that experimental and computational results are deployed in synergistic combination. The reactions of CN and CH radicals, the reactive species of concern here, have been studied using a range of experimental techniques in addition to computational chemistry methods. Because of the complementarity of these studies we now have a good understanding of their reaction mechanisms, an important step toward predicting their reactivity with larger molecules.

3. Results and discussion

3.1. Reactions of the CH radical with unsaturated molecules

The CH radical in its $X^2\Pi$ ground state has been detected in the interstellar medium,[52] combustion environments,[53,54] and under plasma conditions,[55] where it is believe to play a significant role during the chemical growth of carbon molecules. The CH radical is also suggested to be present in planetary atmospheres.[6,7] Its fast kinetics with saturated[56,57] and unsaturated hydrocarbons[14,58,59] indicates a barrier-less entrance channel forming intermediates that may isomerize and dissociate to give the final products. A remarkable property of the CH radical is its ability to react with molecular nitrogen, which is believed to be one of the initial reaction steps leading to the incorporation of nitrogen into hydrocarbon chains.[60-64]

The reactions of the CH radicals with small alkene and alkynes molecules play a significant role in combustion and interstellar chemistry where they contribute to the molecular growth chemical scheme through a CH-addition–H-elimination mechanism. The general mechanism for such reaction can be written as $CH + C_nH_m \rightarrow C_{n+1}H_m + H$ although non H-loss channels are shown to be non-negligible in the

case of the CH + C_3H_6 reaction.[65] In order to better understand the role of these reactions during the molecular growth process it is necessary to identify the hydrogen co-products as well as the contribution from CH_3-loss and other channels.

The reactivity of the CH radial can be attributed to the presence of a singly occupied and one vacant *p*-orbital and the presence of a doubly-occupied partially anti-bonding σ-orbital collinear to the CH-bond. The presence of an unpaired electron in one of the two pure *p*-orbitals of the carbon may lead to doublet-like radical reactivity (i.e. abstraction and addition), while the vacant *p*-orbital and the highest doubly occupied σ-orbital give to the CH doublet ground state ($X^2\Pi$) the structure of a *sp*-hybridized singlet carbene (i.e. addition, cycloaddition, and insertion). The propensity of the CH radical to accept electron pairs in the vacant *p*-orbital may also lead to the formation of a stable dative intermediate.[66]

A better understanding of the chemical role of the CH radical in carbon-rich environments requires differentiating between the different reaction entrance channels for a wide range of molecules and experimental conditions. In the laboratory, ground state CH radicals are produced via debromination of bromoform using 193 nm,[28] 266 nm[14,59,67] or 248 nm[44,68,69] laser photolysis, reaction with potassium atoms,[57,69] or discharge-induced dissociation.[68] Photolytic and discharge dissociations, generate CH radicals with large excess vibrational energy.[68] Quenching to the ground vibrational level can be achieved by collision with a large excess of molecular nitrogen.[67,70] In the case of the reaction with potassium atoms, the CH radicals have been shown to exclusively form in the ground vibrational level.[69] For product detection studies under flow conditions, reactions of the singlet CHBr with the hydrocarbon reactant may lead to the formation of products at the same mass-over-charge ratio than that of the CH reaction products.[71] For photolysis at 248-nm the yield of CHBr formation is found to be negligible compared to that of CH while it is a main photolysis products at 193 and 266 nm.[68,71]

Kinetic and theoretical investigations for the reaction of CH with saturated hydrocarbons have suggested a reaction entrance channel through a single step insertion into C–H bonds to form a substituted alkyl reaction intermediate.[56,57,72] Depending on the size of the carbon chain, this intermediate will decompose either through H-loss to form an alkene or through scission of a C–C bond to from a stabilized alkyl radical + alkene. In the case of reactions with alkenes and alkynes, both the C–H insertion and direct addition at C=C or C≡C bond positions – both carbene-like mechanisms – are calculated to be energetically favorable.[73,74] Insertion into a C–C σ-bond is energetically accessible, although it is likely to be a minor channel compared to the C–H insertion and C=C/C≡C addition due to steric factors. The C–H insertion is predicted to be energetically favorable relative to the π-addition, due to the formation of a resonantly stabilized allyl or propargyl-like intermediate.[44,73] This effect is likely to be countered by the more attractive potential between the radical and the π-electron system.[75] Combined with a larger solid angle for the π-orbital attack compared to that of the σ-orbitals, addition will compete with insertion as a probable entrance channel regardless of the relative stability of the product intermediates. Hydrogen abstraction channels are typically disfavored due to the relatively small exothermicity of the CH_2 + radical product set.

The attack of the CH radical on an unsaturated molecule may result in either addition to a single carbon or cycloaddition to form a 3-carbon atom intermediate, which may either dissociate or isomerize by ring opening. Theoretical investigations based on the quantum mechanical calculation of the minimum energy pathway suggest that the formation of non-cyclic final products generally dominates for energetic and/or entropic reasons, aided by rapid isomerization of any cyclic reaction intermediate to the more stable acyclic isomer.[73] However, these theoretical predictions are in disagreement with experimental studies on the CH + C_2H_2 reaction by Boullart et al.[76] and the unimolecular dissociation of the propargyl radical (C_3H_3) by McCunn et al.[77] both reporting cyclopropenylidene (c-C_3H_2) as the main product. In order to address these discrepancies and to systematically determine the reaction mechanism(s) of CH

radicals with small unsaturated linear hydrocarbons, the CH + C_2H_4, C_3H_6, C_3H_4, and C_2H_2 systems have been studied using isomer-resolved photoionization mass spectroscopy,[44,65] CMB,[27-29] and computational calculations.[44,73,78]

The following paragraphs discuss the most likely reaction mechanisms for reaction of CH with unsaturated hydrocarbons, as well as with nitrogen and oxygen containing molecules, based on experimental isomer identifications. Generally, it is found that the most likely reaction entrance channel depends mostly on the nature of the unsaturated site, while the subsequent isomerizations of the principally formed intermediate depends mostly on the reactant substituents. For this reason a stronger focus is given to discriminating between possible CH reaction entrance channels. Experimental evidence discussed below suggests that cycloaddition and abstraction mechanisms are generally preferred. Although insertion into a σ-bond cannot be totally ruled out, it appears to be minor reaction mechanism for all the investigated reactions.

3.1.1. Reactions with alkenes

The experimental[44,65] and predicted[58] isomer-resolved product branching ratios for the CH + C_2H_4 and CH + C_3H_6 reactions are in qualitative agreement with allene and 1,3-butadiene being the main reaction products, respectively formed after H-loss from CH addition. In the case of the reaction with ethene, discrepancies about the methylacetylene branching ratios are found when comparing flow-tube experiments to CMB data.[28] The difference between the flow tube and the single collision experiments are unlikely to come from the difference in total available energy (3.7 kJ mol^{-1} average thermal energy compared to 17.0 kJ mol^{-1} single collision energy) as all the intermediates and transition states are predicted to be well below the energy of the reactants.[73] In flow tube experiments, collisions with the buffer gas could affect the final branching ratios through stabilization of long-lived reaction intermediates, although this is likely to favor the stabilization of the allyl radical rather than the formation of methylacetylene. In the case of allene and methylacetylene formation, effects of H-assisted isomerization

is likely to be negligible as the activation barrier for the H-atom addition is too high to lead to any significant isomerization at room temperature.[73] RRKM-ME calculations performed on the C_3H_5 potential energy surface would assist in addressing these discrepancies between flow tube and CMB data. In the case of CH + C_3H_6 the detection of 1,3-butadiene as the main reaction product[65] agrees with the predictions from Loison et al.[58] (although they speculatively neglect 1,2-butadiene formation, mostly for energetic reasons). The main discrepancy arises from the non-detection of the CH_3-loss channel in the synchrotron photoionization experiments whereas using H-atom detection, Loison et al.[58] find a 0.78(±0.08) H-atom branching ratio. One possible explanation is that the remaining product fraction(s) – not giving rise to a H atom – may be distributed across several minor channels making their detection challenging.[65] This suggests that the CH_3-loss may not be a major exit channel. All the detected reaction exit pathways in the flow tube experiments are energetically accessible according to the PES calculated by Li et al.[79]

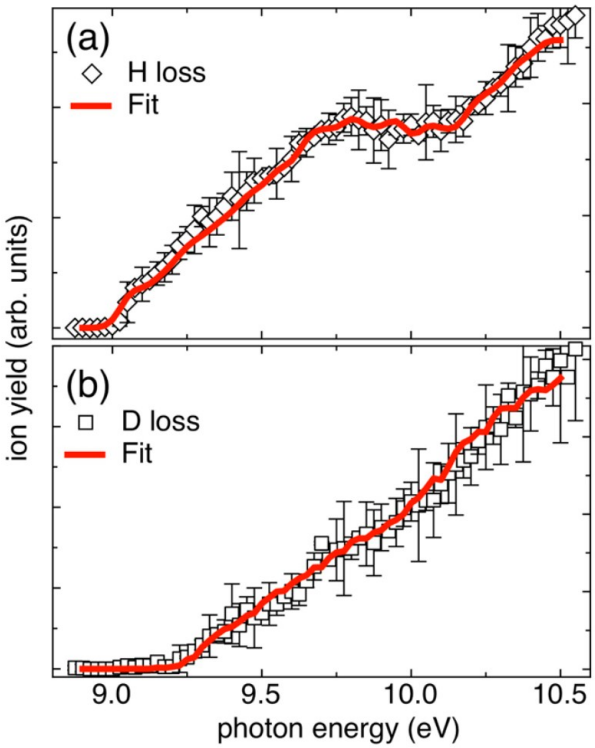

Figure 1 Photoionization spectra for the CD + C_3H_6 reaction at (a) m/z 55 and (b) m/z 54. The red lines are fits to the experimental data from measured isomer reference spectra with (a) 0.89 fraction 1,3-

butadiene and 0.11 fraction 1-butyne and (b) 0.97 fraction 1,2-butadiene and 0.03 fraction 1-butyne. Reprinted with permission from Reference[65]. Copyright (2013) American Chemical Society.

Figure 1 shows the photoionization spectra of (a) m/z 55 and (b) m/z 54 for the CD + C_3H_6 reaction obtained flow tube experiments.[65] In panel (a) the H-loss channel spectrum is fitted with 0.89 fraction 1,3-butadiene and 0.11 fraction 1-butyne. The D-loss channel spectrum in panel (b) is fitted with 0.97 fraction 1,2-butadiene and 0.03 fraction 1-butyne. Similarly, for the CD + C_2H_4 reaction, isotopomeric distributions also identified the D-loss channel as mainly a 1,2-diene molecule, allene.[44] For CH + ethene, cyclopropene may contribute to the total product distribution by no more than 10%. Methylacetylene is the main H-loss product from the CD + C_2H_4 reaction with a non-negligible amount of allene or cyclopropenyl. These isotopomer distributions suggest that 1,2-diene products are mostly formed through elimination of the hydrogen atom initially from the radical while conjugated diene or alkyne through the elimination of a hydrogen atom initially bound to the unsaturated reactant. Scheme 1 displays the most likely reaction mechanism for the formation of 1,2-diene through D-loss.

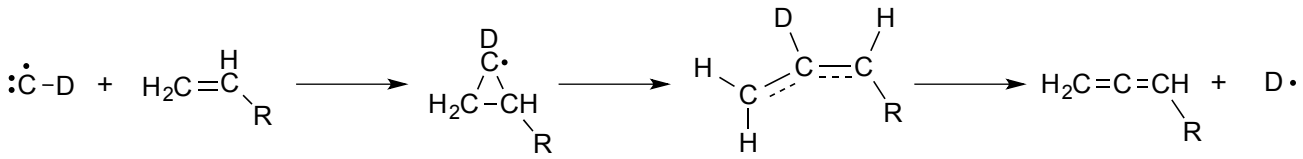

Scheme 1

The radical adds to the double bond to form a cyclic intermediate that immediately isomerizes through ring-opening to form the more stable allyl-like radical. The much higher dissociation barrier for decomposition compared to that for ring opening suggests that formation of cyclopropene should be a minor reaction channel.[28] Several isomerization schemes are possible from the allyl-like intermediate involving 1,2- and 1,3-H/D shifts. The direct elimination of the D-atom initially from the radical is the only exit channel leading to the formation of non-deuterated 1,2-diene and provides strong evidence for the initial cycloaddition mechanism.

Direct insertion of the CH radical into a C–H bond of an unsaturated carbon atom is likely to compete with the cycloaddtion. In the case of the CH + C_3H_6 reaction, the less than unity H-atom branching ratio was used by Loison et al. as evidence for the formation of an isobutenyl radical from direct insertion of the radical into an ethylenic C–H bond which can only decompose through CH_3 loss.[58] As mentioned previously however, the non-detection of the CH_3-loss channel products is at odds with this result.[28,65] The detection of methylacetylene and 1,3-butadiene products, for the CH + ethene and CH + propene, respectively, in both cases retaining the hydrogen atom that originated from the CH radical, can be explained by the formation of an allylic radical intermediate either from direct addition or insertion.[44,65] Overall, direct addition to a carbon atom cannot explain the observed isotopomer distributions unless the initially formed carbene-radical isomerizes through ring-closure to give the cyclic intermediate. Entrance channels other than cycloaddition do not need to be invoked to explain experimental reaction product identifications, although they cannot be unequivocally ruled out.

For the CH + allene reaction,[44] the detection of both 1,2,3-butatriene and vinylacetylene is consistent with an initial CH cyclo-addition on the π-electron system of allene to form a cyclic intermediate which can isomerize through ring-opening to the more stable 1,2-butadiene-4-yl radical. In the absence of isotopic labeling experiments it is not possible to discriminate between cycloaddition and direct insertion. Loss of the hydrogen initially from the CH radical would form 1,2,3-butatriene while elimination of a terminal H-atom initially residing on allene forms vinylacetylene. Insertion into one of the C–H bonds could also lead to the observed products.

Additional evidence for the cycloaddition of the CH radical onto C=C double bonds was inferred from the isotopomer distribution of the CH + pyrrole reaction.[80] Scheme 2 displays the most direct reaction mechanism leading to ring expansion.

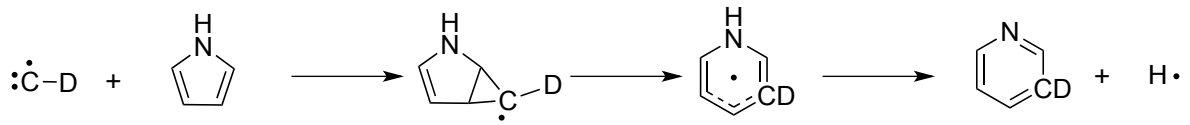

Scheme 2

The detection of only pyridine as a reaction product suggests that the initially formed reaction intermediate isomerizes through ring expansion to give a six-membered aromatic ring. The substitution of the hydrogen from the radical by a deuterium atom leads to a shift of the product mass by one unit. The formation of the pyridine therefore proceeds solely through the loss of the hydrogen atom initially from the pyrrole ring. The CH radical is likely to add to the π-system of the aromatic to form a bicyclic intermediate. The bicyclic intermediate isomerizes by ring opening to form a six-membered ring. As the H is lost from the N-site exclusively, the pyridine product contains the hydrogen atom initially from the radical. This H elimination must be rapid as there is no evidence of H-atom scrambling in the deuterium labeling experiment.[80]

The isotopomer product identifications for the CH reactions with ethene, propene and pyrrole provide strong evidence that the radical cycloaddition onto the C=C bond is a major entrance channel. This mechanism is also consistent with the CH + allene reaction products. The C—H σ insertion mechanism is likely to play a less significant role for these reactions. The relative importance of the addition versus insertion entrance channels for the reaction of CH with ethene and its derivatives can be conceptualized using orbital correlation between the radical and the reactant. By analogy with the sp^2-hybridized singlet CH_2 carbene,[75] the CH radical is likely to react through electrophilic addition onto occupied σ- and π-orbitals of the reactants. Figure 2 shows the most likely geometry for the transition state of the initial CH encounter with the π-orbitals of ethene leading to (a) addition and (b) insertion.

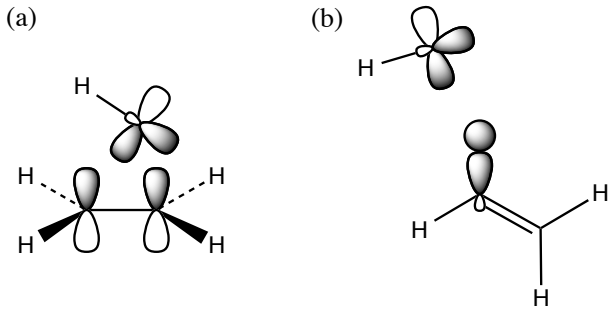

Figure 2 Attack of the CH radical for (a) cycloaddition and (b) insertion into ethene. The singly occupied orbital of the radical is not represented.

These transition states are based on molecular orbital correlation and *ab initio* calculation for the singlet CH_2 attack on ethene and are adapted here for the CH radical.[81-85] For clarity the singly occupied *p*-orbital is not depicted. In Figure 2 (a) the addition of the radical onto the double bound occurs through a concerted off-center overlap of the vacant *p*-orbital with the π-orbital together with an overlap of the doubly occupied σ-orbital with the $\pi*$-orbital of the reactant.[81,83,85] The initial encounter complex will rearrange through rotation of the added C–H to create two new σ-bonds and form the cyclopropenyl radical. As shown in Figure 2 (b) the approach of the reactants for insertion into a C–H bond is likely to occur via interaction of either the vacant or the singly occupied *p*-orbital with the hydrogen atom.[82,86] The transition state is adapted from *ab initio* calculation for the singlet CH_2 insertion into methane.[82] The formation of a three-centered transition state in which the carbene interacts with both the carbon and the hydrogen atoms was not found in the potential energy surface of the $CH_2 + C_2H_2$ reaction.[82] In the case of $CH + H_2$, a similar approach as that depicted in Figure 2 (b) is predicted, although the CH and H_2 bond are parallel.[86] Following the initial approach, the hydrogen atom will transfer to the electron deficient carbon before the system collapses to the insertion intermediate. Although direct abstraction may occur through a similar interaction of the reactants, it is often endothermic, while the insertion is exothermic and barrierless. The fact that the insertion mechanism requires a side interaction with the hydrogen compared to the planar p-π interaction for addition is likely to favor the CH addition over C–H insertion. The interaction of the singly occupied *p*-orbital with both the π and π*-orbitals of the reactant may also lead to

addition onto one of the unsaturated carbon atoms[87] although there is no strong experimental evidence of such a mechanism in the case of the reaction with alkenes presented here.

3.1.2. Reactions with alkynes

Figure 3 displays the photoionization spectrum of m/z 38 from the CH + C_2H_2 reaction obtained by integrating the ion signal from 20 ms to 80 ms after the laser pulse. The blue thick curve is the Franck-Condon simulation of the cyclopropenylidene photoionization spectrum fitted to the experimental data. For comparison, the Franck-Condon simulation of the triplet propargylene is normalized to the experimental spectrum.

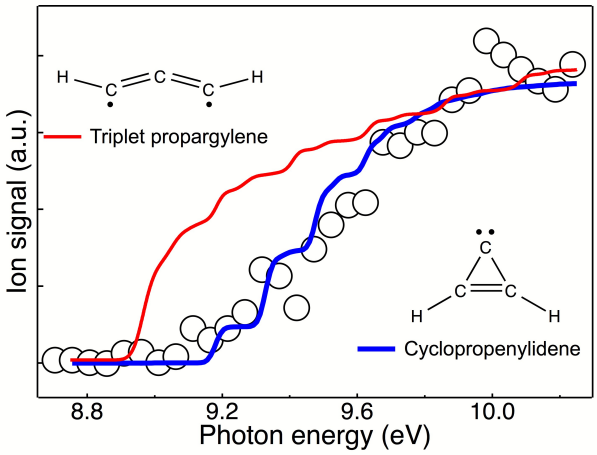

Figure 3 Photoionization spectra for the CH + C_2H_2 reaction at m/z 38 integrated from 20 ms to 80 ms after the laser pulse. The red line is the Franck-Condon simulation of triplet propargylene and the blue line the Franck-Condon simulation of cyclopropenylidene. Reprinted with permission from Reference[44]. Copyright (2009) American Chemical Society.

The experimental detection of c-C_3H_2 under thermal conditions agrees with RRKM-ME calculations performed on the CBS-APNO potential energy surface displayed in Figure 4 at 300 K and 4 Torr.[44] The cycloaddition, addition to a single carbon, and the C–H insertion mechanisms are all predicted to be barrierless. Any of the initially formed intermediates may further isomerize to the more stable propargyl

radical through transition states all below the energy of the reactants. The propargyl radical can then either be stabilized by collisions with the buffer gas or decompose to triplet-propargylene (C_3H_2).

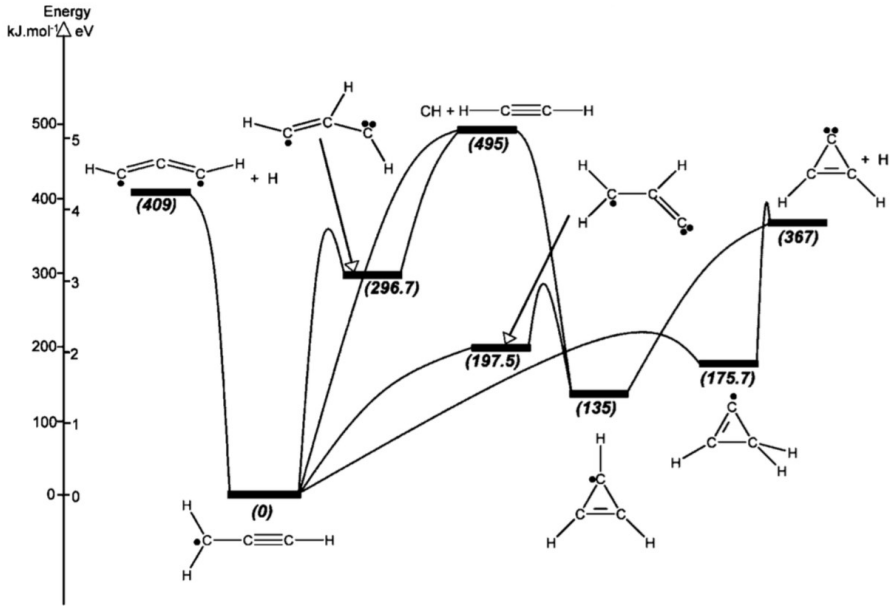

Figure 4 C_3H_3 potential energy surface calculated using the CBS-APNO method. Reprinted with permission from Reference[44]. Copyright (2009) American Chemical Society.

Spectra comprising reaction times up to 20 ms after the laser pulse show a small contribution (<10%) from the triplet propargylene. Time- and isomer- resolved product detection demonstrated that a large amount of the cyclic product was formed through H-assisted isomerization of the triplet-propargylene. H-atom produced by photodissociation and reactions can add to the triplet product without any activation energy to reform the propargyl radical with a lower internal energy. Ultimately this process shifts the product distribution toward the formation of the most thermodynamically favorable isomer. The isotope labeling of hydrogen atoms was unable to provide further mechanistic information due to strong isotope effect of the isomerization scheme of the C_3H_2D system.

CMB experiments at 16.8 kJ mol^{-1} collision energy report the formation of 31.5(±5.0)% of cyclic C_3H_2, 59.8(±5.0)% of acyclic isomer and 9.0(±2.0)% of C_3H through H_2 elimination. Maksyutenko et al.[29] predict that the reaction proceeds through the indirect formation of the propargyl radical and unimolecular

dissociation to form the linear propargylene or the linear C_3H isomer. The c-C_3H_2 product is formed through H-loss from the cyclopropenyl radical. The cyclic intermediate may be formed either by direct cycloaddition or addition to a single carbon and insertion followed by closing of the ring. Evidence for the addition mechanism was inferred from the isotopomer identification from the CH + C_2D_2 reaction.[27] The insertion of the CH radical onto a C–D bond of acetylene forms the HDCCCD radical. Direct molecular hydrogen-loss forms HD + CCCD while the formation of D_2 + CCCH requires the formation of a DDCCCH intermediate. The detection of HD and D_2 with a 1:1 ratio suggests that these intermediates are formed in equal amount likely through an indirect reaction channel rather than through direct insertion. As reported by Kaiser et al.[27] this finding agrees well with the absence of primary kinetic isotope effect for the CH + C_2D_3 reaction.[88] Overall the H/D-loss channels are consistent with cycloaddition while the H_2/HD/D_2 distribution suggests addition into a single carbon. The 9 to 13% branching ratio for the formation of molecular hydrogen[27,29] suggests that the addition onto a single carbon is less probable that the cycloaddition.

Product detection studies of the CH + methylacetylene reaction provides further evidence for the formation and direct decomposition of a cyclic intermediate. Contrary to the reaction with its isomer allene, reaction with methylacetylene leads to facile formation of cyclic products with low ionization energies.[44] Cyclic isomers represent up to 30% of the total detected reaction products. The photoionization spectra of the H-loss products methylenecyclopropene and cyclobutadiene are very similar and thus do not allow the determination of the exact structure of the cyclic isomer. The formation of methylenecyclopropene could be explained by direct addition onto the triple bond followed by the loss of a hydrogen-atom initially from the methyl group. The reaction is also found to form the linear H-loss co-product vinylacetylene. Part of the C_4H_4-ion signal was attributed to the formation of 1,2,3-butatriene.[44] It is however possible that this signal comes from shape resonances in the spectrum of the cyclic isomer not accounted for by the Franck-Condon calculations. The branching ratio for the formation of the triene is

therefore likely to be much lower than that reported by Goulay et al.[44] Vinylacetylene is likely to be formed by C-H insertion of the CH radical into the methyl group.

The product detection results for CH + C_2H_2 and the corresponding isotopologue (C_2D_2), together with the detection of cyclic isomers for the reaction of CH + methylacetylene, strongly suggest that the addition of the radical onto the acetylenic bond through the simultaneous attack on both orthogonal π-orbitals is the major reaction entrance channel. Addition to a single carbon may account for up to 13% of the entrance channel in the case of acetylene.[27,29] The insertion into an acetylenic C–H does not appear to compete with insertion into an alkyl substituate C–H bond when it is present.

3.1.3. Reactions with carbonyl molecules

Carbonyl containing molecules are present in combustion environments as fuel (e.g. biodiesel), fuel additives (e.g. acetone), or as combustion intermediates and products. Their reaction with carbon-containing radicals such as CH is likely to affect the early stage of the thermal transformation process, when the CH radicals are abundant. A better understanding of reactions between carbonyl-containing species and combustion radicals in important for optimizing alternative-fuel combustion with the ultimate goals of reducing unwanted emissions while increasing energy-efficiency. The reaction mechanisms of the CH radical with molecules containing a carbonyl group (C=O) have been investigated at room temperature by isomer-resolved product detection, including deuteration studies, of CH + CH_3CHO and CH + CH_3CH_3CO.[71,89] Both reactions are found to lead to the formation of substituted ketenes (containing the C=C=O group) and conjugated enals (C=C–C=O) by H-loss. The detection of ketene and the ethyl (C_2H_5) and acetyl (CH_3CO) radicals in the case of CH + acetaldehyde also suggest minor CH_3, HCO and CH_2-loss pathways. Figure 5 shows the photoion spectra of (a) m/z 70 (D-loss) and (b) m/z 71 (H-loss) for the CD + acetone reaction.[71] In panel (a) the H-loss channel spectrum is fitted with the spectrum of dimethylketene. The ethylketene spectrum (an isomer of dimethylketene, green thin line in Figure 5) is poorly matched with the experimental data close to the ion onset. The D-loss channel spectrum in panel

(b) is well-fit by the spectrum of methacrolein. Similarly, in the case of CD + acetaldehyde the D-loss channel entirely partitions to the substituted ketene isomer while the H-loss channel exclusively forms the conjugated enal.[89]

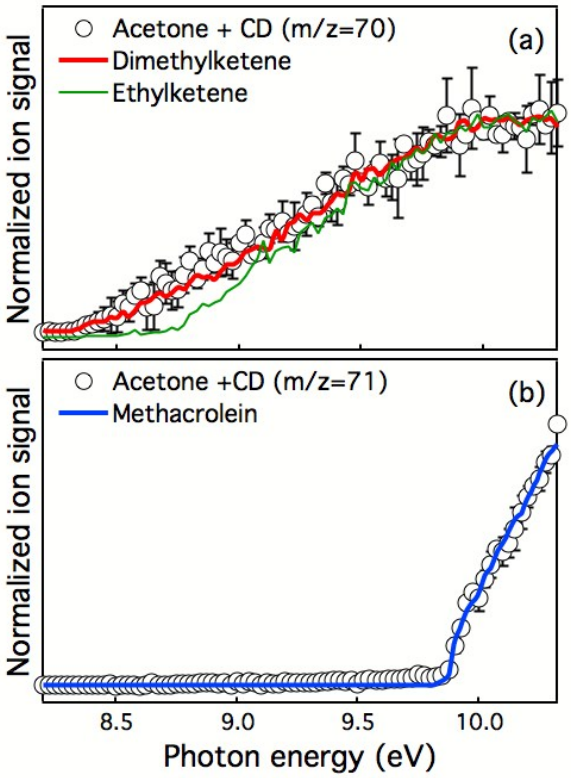

Figure 5 Photoionization spectra of (a) m/z = 70 and (b) m/z = 71 from the CD + acetone reaction. The thick red line in panel (a) is a fit to the experimental data including only contribution from the photoionization spectrum of dimethylketene. The green line is the spectrum for ethylketene superposed on the experimental data. The blue line in panel (b) is a fit to the experimental data including only contribution from the photoionization spectrum of methacrolein. Reproduced from Ref. 71 with permission from the PCCP Owner Societies.

As shown in Scheme 5, following the initial cycloaddition attack of the CH radical, the results comply with (i) the reaction intermediate decomposing to form a substituted ketene by loss of the hydrogen atom initially from the CH radical and (ii) a conjugated enal by loss of a hydrogen atom initially from the carbonyl reactant. In addition, the formation of acrolein through D-loss in the case of CH + CD_3CHO

suggests that conjugated enals are formed by the loss of a H atom originating from the $-CH_3$ group of the carbonyl molecule.

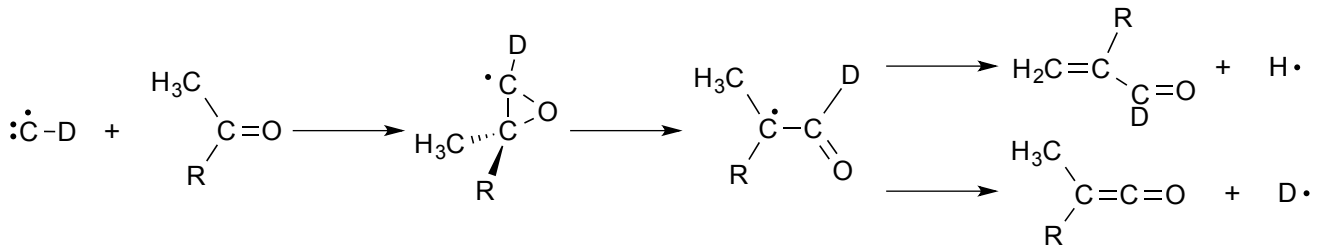

Scheme 5

The detection of the acetyl radical (CH_3CO) by reaction of the CH radical with acetaldehyde suggests that direct abstraction from the H-atom on the carbonyl group is a favorable channel. The absence of the abstraction product in the case of acetone may be explained by the higher bond energy of the methyl C–H bond (388.3 ± 9.2 kJ·mol^{-1}) relatively to that of the acetyl C–H bond in acetaldehyde (358.6 ± 9.6 kJ mol^{-1}).[90] Insertion of the CH radical into a methyl group C–H bond of acetaldehyde is consistent with formation of ethyl + CO, ketene + methyl, and acrolein + H. However, this mechanism does not explain the formation of either the formyl + ethene channel or the methylketene + H channel. Ultimately, no evidence for an insertion mechanism is found for the CH + acetone reaction. This general mechanism is in agreement with recent quantum chemical calculations for the CH + H_2CO reaction[78] where it is predicted that the main room temperature pathway is addition of the radical to the carbonyl group, either by cycloaddition or carbon addition, followed by isomerization to give ketene + H.

The bonding orbitals of the carbonyl group in acetone and acetaldehyde are similar to those of an ethylenic bond although the carbon atom is more electropositive than the oxygen atom. The CH radical is likely to attack the C=O through transition states similar to that depicted in Figure 2 for ethene. The position of the radical relative to the two atoms of the CO group may be more off-centered due to the asymmetric density of charge on carbonyl group. A nucleophilic attack of the doubly occupied orbital of the CH onto the electropositive carbon atom would lead to an addition intermediate that is likely to isomerize through ring closure, as calculated for the CH + H_2CO reaction.[78] Attack of the C–H bond by

the CH radical through a transition state similar to that depicted in Figure 2 (b) for ethene will lead to insertion as well as abstraction of the acetyl hydrogen due to the lower bonding energy. In the CH + H_2CO case, insertion is calculated to be more than one order of magnitude slower than the addition channels over the 300 to 1000 K temperature range.[78] This prediction qualitatively agrees with the small branching ratios measured for the insertion channels in the case of CH + acetaldehyde.

Studies of CH/CD + acrolein, a reactant with both a C=C site and a C=O site, also suggest that the entrance mechanism proceeds predominantly via cycloaddition of the CH radical onto either unsaturated site.[91,92] The most compelling evidence for this mechanism is the detection of furan only via H-loss, which is consistent with both cycloaddition onto the vinyl or carbonyl unsaturation. For both reaction intermediates, ring-opening leads to a stable conjugated radical. Although H-loss from this intermediate to form 1,3-butadienal is entropically favorable compared to the ring closure, the energy barrier for the formation of the furan-H adduct is lower by about 115 kJ mol^{-1}. Addition to the terminal carbon atom of acrolein and insertion mechanisms probably also play a part in the reactivity and may explain the apparent C_2H_2O and C_3H_4 formation or minor products of the H-loss channel.

3.1.4. Predicting reaction mechanisms with larger molecules

Following from systematic studies of the reactions between the CH radical and several small prototypical unsaturated molecules mechanistic trends emerge which can be used to predict the CH reactivity with other unsaturated species. The reaction of the CH radical with large unsaturated molecules is likely to be governed by the electrophilic interaction of the vacant *p*-orbital on CH with the occupied σ- and π-orbitals of the reactants as well as the interaction of the doubly occupied σ-orbital on CH with reactant π^*-orbitals. Experimental evidence presented in this perspective strongly suggests that the cyclo-addition onto C=C and C=O bonds will play a major role with minor effect of the substituents. By analogy with the reactions of the singlet CH_2 carbene, the C–H insertion mechanism is likely to be less favored when compared to cycloaddition although it will become more significant as the length of the carbon chain increases for

statistical reasons. This trend is likely to be applicable to the reaction with larger hydrocarbons that have not been investigated experimentally or theoretically. The reaction with alkene and alkyne will mostly lead to conjugated-diene products with a non-negligible fraction of three-atom cycles product in the case of alkynes. Reaction with long saturated carbon chains will also lead to alkene formation through C–H insertion. The reaction with carbonyl containing molecules will mostly form substituted ketenes and conjugated enal products. In the case of ester functional groups, such as those found in biodiesel molecules, the reaction products are likely to be similar to those produced by the reaction with ketones. Because of the long carbon chain, insertion products will also be present. In the case of the reaction with nitrogen-containing molecules, the most likely reaction entrance channel of the CH + NH_3 reaction is found to be the formation of a dative bond by direct interaction of the empty *p*-orbital on CH with the lone electron pair in the σ-nonbonding orbital of the nitrogen atom.[66] If this mechanism is the main entrance channel, the reaction of the CH radical with larger methyl-substituted amines is likely to lead to the formation of methylimine functional groups. Linking to Titan's gas-phase chemistry, ammonia and cyanogen-containing molecules are included into models,[93] and primary amines as well as nitrogenated polycyclic aromatic hydrocarbons have been identified in laboratory tholins.[94,95] The facile addition-elimination of the CH radicals onto a nitrogen containing group suggests that such reactions may play an important role as a pathway to incorporate atomic nitrogen in the carbon chemical growth mechanism.

3.2. Reactions of the CN radical with alkenes and aromatic molecules

The formation and reactions of the CN radical are important for the chemistry of many different reacting environments. While the kinetics of CN + hydrocarbon reactions are generally well-studied there are fewer product detection studies and certainly very few product studies at different temperatures. The kinetics of the CN radical have been well investigated - a recent summary of kinetic data for CN reactions with C_2H_2, C_2H_4, C_3H_6 and trans-butene and iso-butene are found in Gannon et al.[96] Very low temperature rate coefficients of CN reactions with a range of small linear hydrocarbons are reported down to 23 K using Laval nozzle expansion techniques.[16] The rate of reaction is governed by long-range interactions and these reactions occur essentially at the collision rate limit. Since in many cases there is no barrier on the entrance channel, such CN reactions are relevant to understand the formation pathways of nitriles and other N-containing species in cold environments – this includes planetary atmospheres (e.g. Titan and potentially: Triton and Pluto[16]) and, the interstellar medium.[97] In the astrochemical context, the production of CN radical is generally attributed to the photolysis of HCN.[98] For higher temperatures, experimental techniques have measured kinetics of CN reactions with small linear hydrocarbons up 1200 K.[17,18] In combustion chemistry, the CN radical is a key species in the incorporation of nitrogen into large carbon structures and is also implicated in the fate of NO and many other reactions.[64] Nitrile species are also important in the combustion of biofuels.[99] All these aforementioned chemical systems require accurate knowledge of product branching ratio for elementary CN + hydrocarbon reactions.

Mechanistically, it is generally accepted that CN radical will react with unstaturated hydrocarbons by direct addition to unsaturated carbons forming radical intermediates that, at low pressures, will dissociate by loss of a small neutral fragments – usually H atoms or, if suitable pathways exist, CH_3 radicals. The mechanism of H atom loss can vary depending on the structure of the reactant molecules. As will be shown herein, the general $CN + C_xH_y \rightarrow C_{x+1}H_{y-1}N + H$ reaction scheme for CN reactions with small unsaturated hydrocarbons does not always account for the total product set. Furthermore, the nitrogen-

containing co-product(s) of H-loss may include a considerable number of thermodynamically plausible isomers. Recently, a number of experimental studies are reported, using several experimental strategies, to detect and measure products from CN + hydrocarbon reactions. Coupled with computational studies, with kinetic modeling and product branching predictions, these investigations have enabled a deeper understanding of reaction mechanisms. In what follows, several CN reactions are details with emphasis on isomer specific product detection.

3.2.1. CN + ethene.

The CN + C_2H_4 rate coefficients have been reported for a large range of temperatures including down to 25 K [96,100] and up to ~1200 K.[18] The 298 K rate coefficient is reported to be 2.5×10^{-10} cm^3 $molecule^{-1}$ s^{-1} [101] indicating essentially unity reaction efficiency. With detection of H atom product quantum yields of one, as determined by quantitative H atom laser-induced fluorescence,[101] this study points to C_3H_3N + H as the dominant product set. Seakins and coworkers utilized the same H atom LIF technique to monitor the time-dependent H-atom product yield in tandem with CN disappearance LIF and found the rate coefficients determined by both techniques to be in good accord; the 298 K H atom LIF rate coefficient is reported as $3.21 \pm 0.62 \times 10^{-10}$ cm^3 $molecule^{-1}$ s^{-1} and the 298 K CN LIF rate coefficient $2.91 \pm 0.18 \times 10^{-10}$ cm^3 $molecule^{-1}$ s^{-1}. This study also includes a computational RRKM analysis to predict the products and rationalize the experimental measurements. The key finding concerning reaction products is the prediction that the C_2H_3CN species (cyanoethene) is the dominant H atom co-product, from an addition then H atom loss process.

CMB experiments by Balucani et al. probed (electronic ground state) CN reacting with ethene at collision energies of 15.3 and 21 kJ mol^{-1}.[31] The study reports that CN + ethene exclusively produced cyanoethene by CN addition followed by H (^2S, ground state) atom elimination via a relatively long-lived intermediate (longer that its rotational period). No evidence for a direct H abstraction pathway, forming HCN + C_2H_3, was reported in these studies. At low pressures, computational results with RRKM analysis

from Vereecken et al.[102] predict that HCN production from addition/elimination channels should remain <1% at temperatures <1000 K and that any significant direct H-abstraction may only contribute at temperatures > 1200 K. They caution that these predictions depend on a tentatively assigned 10 kJ mol^{-1} direct H atom abstraction barrier. The Vereecken *et al*. study also predicts that at low temperatures (~300 K) and pressures below 10^4 Pa, the CN addition followed by H-elimination pathway should dominate, >90%. Recently, a CMB study investigated this reaction at very high collision energy (42.7 kJ mol^{-1}) and reported evidence of isocyanoethene (H_2C=CHN=C) product formation.[103] This study points out that previous CMB studies were conducted at significantly low collision energies such that the iso-cyano product channel is not accessible.

Synchrotron photoionization mass spectrometry experiments have been performed for CN + C_2H_4 reaction generating CN from 248 nm laser photolysis of ICN under conditions of 4 Torr and 298 K.[104] The product mass spectrum acquired at 11.05 eV photoionization energy shows one clear peak at *m/z* 53, consistent with production of a C_3H_3N species – the time dependence of this signal, relative to the CN photolysis laser pulse, shows a fast rise followed by a constant signal up to the measured 80 ms time duration.

The photoionization spectrum of the *m/z* 53 signal has an onset at about 10.9 eV in good agreement with the calculated adiabatic ionization energy (AIE) (CBS-QB3, 10.90 eV) and measured AIE (10.91 eV, NIST)[105] of cyanoethene. There is no signal that would suggest any significant C_2H_3 radical (*m/z* 27) formation from a H-abstraction pathway and this channel is ascribed a <2% branching limit. Using this experimental arrangement to detect HCN directly from this reaction is difficult as HCN has a relatively high AIE (13.6 eV) such that the detector would be overwhelmed by signal from all other ions. Regardless, computational predictions and our experimental attempts to detect C_2H_3 are in agreement with other studies that affirm that the HCN + C_2H_3 channel is very minor at these conditions. Scheme 4 displays the dominant reaction channel for the CN + C_2H_4 reaction.

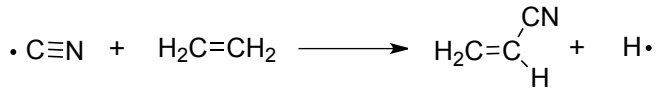

Scheme 4

Computational studies on the reaction mechanism have indicated that there are two plausible channels from the direct CN + C_2H_4 addition intermediate, the CH_2CH_2CN radical:[106,107] (i) direct H-loss to form cyanoethene (CH_2=CHCN) (acrylonitrile) or (ii) a 1,2 H atom shift to form CH_3CHCN that can then undergo H-loss from the methyl group to form the same cyanoethene product. The end product of the two possible pathways is the same (Scheme 4). The synchrotron photoionization experiment provides no information on the intermediate pathway to the detected products. Kaiser and Balucani report,[106] from RRKM calculations, that 40% of cyanoethene is formed from the (i) direct fragmentation of the CH_2CH_2CN intermediated and 60% from the (ii) decomposition of the second CH_3CHCN intermediate.

The photoionization spectrum of the *m/z* 53 product shows no evidence for the production of the iso-cyanoethene (CH_2CH-N=C) species as the AIE of this isomer is calculated (CBS-QB3) to be 10.56 eV and no ion signal is detected until 10.9 eV. Calculations are in agreement with this finding, revealing that the H-elimination transition state from a CH_2CH_2NC is placed +12 kJ mol^{-1} above the entrance channel energy of the reactants. As mentioned above, the only evidence for this channel is recorded in CMB for which the collision energy (42.7 kJ mol^{-1}) is much higher than the CH_2CH_2NC exit barrier.[103]

3.2.2. CN + propene and larger linear unsaturated hydrocarbons

Extending the CN reaction partner from ethene (C_2H_4) to propene (C_3H_6) significantly increases the number of plausible reaction pathways and products. Numerous research groups have studied the CN + C_3H_6 reaction with various experimental and computational techniques. The CN + propene rate coefficient is measured at 3.18 ± 0.21 × 10^{-10} cm^3 $molecule^{-1}$ s^{-1} [96] which again points to unity reaction efficiency. Using H atom LIF product detection, Seakins and coworkers[96] reported that at 298 K the H atom product yields were pressure dependent spanning yields of 0.478 at 2 Torr down to almost zero at 200 Torr (in He buffer gas). These results are rationalized, using RRKM modeling, as the result of some stabilisation of

the CN-C_3H_6 addition intermediate. For this reaction, there are three plausible H atom co-product isomers with the C_4H_5N formula: 1-cyanopropene, 2-cyanopropene and 3-cyanopropene (shown in Scheme 5). Other experiments, described below, have provided details on the product ratios. The remaining question is what accounts for the non-H atom product yield. From calculations, a CH_3 + C_3H_3N exit pathway is energetically plausible and a zero-pressure CH_3 elimination yield of 0.51 is predicted at 298 K.[96] The high-precision measurements of the H atom appearance kinetics are vital to understand the underlying mechanism of the reaction but further experimental investigation is required to elucidate the structure(s) of the H-atom co-product and characterize the C_2H_3CN + CH_3 product channel.

CMB studies of CN + propene have been performed utilising deuterated propene analogues to distinctly probe the product channels.[30] At collision energy of 25.5 kJ mol^{-1}, CN reactions with the (i) CH_2=$CHCD_3$ and (ii) CD_2=$CDCH_3$ isotopologues both gave rise to a signal at *m/z* 70 that is due to CN addition followed by H atom (1 Da) loss. As the H atom loss channel was observed for both isotopomers, cases (i) and (ii), it shows that there is more than one distinct H atom loss product mechanism. The CMB study ultimately reports a 75% (± 8) *cis*/*trans*-2-butenenitrile (1-cyanopropene) product yield for the CN + CH_2=$CHCD_3$ reaction and 25% (± 5) for 3-butenenitrile (3-cyanopropene) in the CN + CD_2=$CDCH_3$ reaction.

A CN + propene computational study by Huang *et al*. pointed out that the product distribution for this reaction depends to a significant extent on the entrance channel of CN forming different CN–propene adducts.[108] Regardless of the intermediate however, their ultimate finding is that the CH_2=CHCN + CH_3 pathway will be dominant (always greater than 50%) at low collision energies (0 – 21 kJ/mol) and the H atom co-product species are predicted to comprise 1-cyanopropene and 3-cyanopropene, in accord with the aforementioned CMB study.

Two synchrotron product detection studies have focused on the CN + propene reaction. The first, reported the cyanoethene (CH_2=CHCN) + CH_3 channel as the dominant pathway and the H loss pathways was apportioned to 1-cyanopropene and 2-cyanopropene.[104] For these cyanopropene isomers, the fitting relied on simulated photoionization spectra. Subsequently, the acquisition of further experimental data led to revision of this finding. With the benefit of a higher experimental mass resolution and experimentally determined photoionization reference spectra for the three cyanopropene isomers, the updated result still assigns cyanoethene + CH_3 channel as the dominant product channel (0.59 ± 0.15) and the H loss channel accounts for the remaining product yield (0.41) but the H-loss co-product species are assigned as 1-cyanopropene (0.50 ± 0.12) and 3-cyanopropene (0.50 ± 0.24). The study points out that although these reported fractions represent the best fit to the experimental data, the close similarities between the photoionization spectra of the three cyanopropene (C_4H_5N) species leaves some uncertainty around the equivocalness of this assignment. Further experiments in the same study for deuterated analogues provides additional evidence for the formation of 3-cyanopropene. The CN + CH_2=$CHCD_3$ reaction was studied and it revealed that both a D atom loss (-2 Da) and H atom loss (-1 Da) product channels were present. The detection of the D loss channel is sound support for the formation of 3-cyanopropene (as illustrated in Figure 6 from data reported in Ref [109]) along with the earlier fitting results to the product photoionization spectrum. These studies, including CMB[30] and more recent calculations[108] are in accord with the finding that 1-cyanopropene and 3-cyanopropene are the major products of the H-loss.

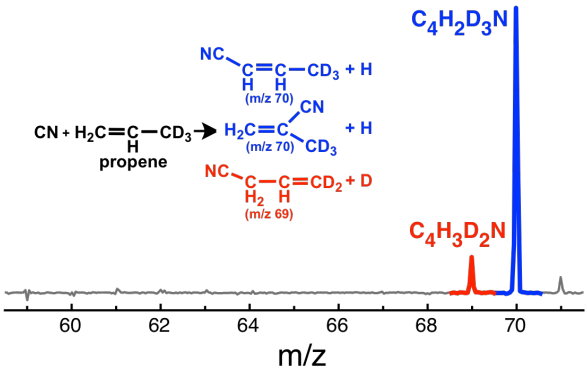

Figure 6. Product mass spectrum of the CN + propene-d_3 reaction that shows evidence for both D and H elimination. Reprinted with permission from Reference[109]. Copyright (2011) American Chemical Society.

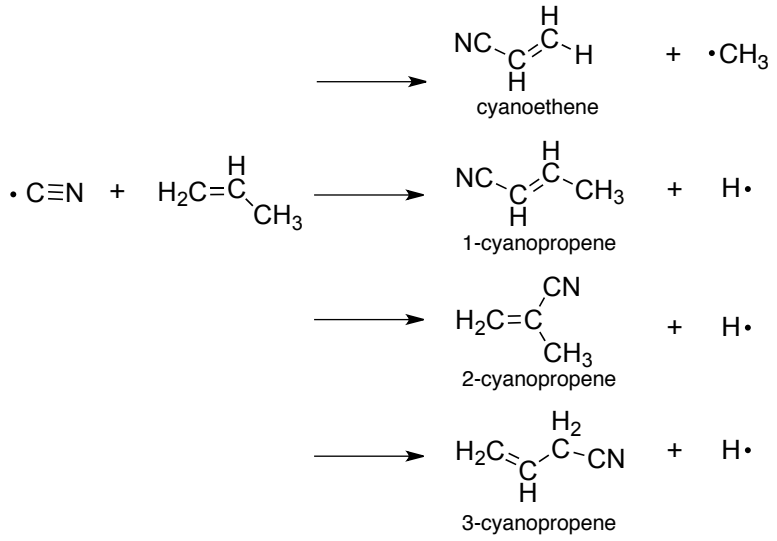

Scheme 5

In a final comment on this reaction, there is a recent study of the CN + 1-pentene reaction by Suits and coworkers using crossed-beam imaging at collision energies from 21 to 38 kJ mol^{-1} in which they clearly detect an HCN abstraction channel, forming the C_5H_9 radical co-product.[110] The authors conclude that the HCN channel is not insignificant and cautiously report a branching contribution of 50%. So perhaps there is an unresolved question on the possible presence of this HCN abstraction channel for the case with propene. In the CN + propene studies using synchrotron photoionization mass spectrometry mentioned above, deliberate experiments were performed in an effort to detect the analogous radical for the CN + propene reaction C_3H_5 – the resonance-stabilized allyl radical – with no definitive detection at the corresponding *m/z* 41. So there might be some unidentified dynamics and nuisances in the H atom abstraction pathway that opens this channel in the case of 1-pentene but renders it uncompetitive for the case of propene.

As explored computationally by Mebel and coworkers, extending CN radical reactions to larger chain olefin species may lead primarily to "CN-for-H exchange" reactions (C_xH_y + CN -> $C_xH_{y-1}CN$ + H) as in the case of CN + C_2H_4, but competition with other elimination pathways, including those with available

CH_3-loss and C_2H_5-loss channels, need to be carefully considered.[111] This is clear from the CN + propene example explained above. Experiments, CMB and low temperature kinetics (298 – 23 K) are reported for the CN + 1,3-butadiene reaction. In this case the "CN-for-H exchange" holds true, with 1-cyano-1,3-butadiene established as the dominant product.[15] Only traces of pyridine are detected.

For other C_4H_6 reaction partners, computational investigations for CN + 1-butyne predict that CH_3 elimination and H elimination product pathways are both important and the fractionation is sensitive to the initial CN adduct site.[111] The CN + 1,2-butadiene reaction is also predicted to follow CH_3-loss and H-loss product channels following CN addition, although H loss is predicted to be preferred.[111] The CN + 2-butyne reaction is predicted to give >98% 1-cyano-prop-1-yne + CH_3 products across 0-5 kcal mol^{-1} (0-21 kJ mol^{-1}) collision energies. For these C_4H_6 species, various product detection schemes, including synchrotron photoionization mass spectrometry, would provide important experimental insight into any preference for the various entrance channels. Take the CN + 1,2-butadiene reaction as a particular example, as the Jamal and Mebel study details, there are three plausible CN addition sites to CH_2=C=CH-CH_3 that form distinct initial intermediates. An addition to the =C= carbon at collision energies 0-5 kcal mol^{-1} (0-21 kJ mol^{-1}) is predicted to ultimately yield almost exclusively 2-cyano-1,3-butadiene + H products.[111] Other adduct sites, at the CH_2 group or the CH group of 1,2-butadiene should generate 1-cyano-prop-3-yne + CH_3 and cyanoallene + CH_3, respectively with yields that are dependent on the collision energy. Isomer specific detection of cyanoallene (up to ~45%) appears predicated on the formation of CN adduct to the CH carbon while 1-cyano-prop-3-yne (up to ~74%) signifies a CN adduct complex at the CH_2 carbon. 2-Cyano-1,3-butadiene makes up the remaining product fraction. It is possible that measurements of product branching ratios will provide insight into the addition process. Judicious deuterium labeling experiments would also provide complementary details to this system, and similar cases, too. As is the case for CN + 1,2-butadiene, the products of CN + 1-butyne and 2-butyne reactions have not been comprehensively studied experimentally with isomer-specific detail. It is not yet clear if

there are any preferential entrance channel dynamics affecting these reactions. Experiments with isomer-specific detection capabilities are required to assist in answering these questions.

Finally, the reactions between small radicals and linear hydrocarbon molecules may lead to ring formation. These processes are of particular interest as ring proliferation is required for the formation of larger PAH/PANH scaffolds that can ultimately condense to form aggregates and particles. One example of a ring formation reaction is the C_2H + 1,3-butadiene reaction that has been shown, under single collision conditions to form benzene + H at 40% product yield.[4] For the analogous CN + 1,3-butadiene reaction, however, no ring-closure pathways to pyridine are significantly competitive – only traces of pyridine are reported – due to high reaction barriers compared to linear isobaric species.[15] As shown in the next section, CN does rapidly react with aromatic species and is implicated in high order ring-formation mechanisms.

3.2.3. CN + benzene, toluene and other aromatics

The reactions of the CN radical leading to larger CN containing aromatics, starting with CN + benzene, are well studied. Kinetics for this reaction have been measured at 105 K, 165 K and 295 K and the rate coefficients are essentially unchanging over this temperature range with values between 3.9 and 4.9 × 10^{-10} molecule^{-1} cm^3 s^{-1}.[112] These results are in good agreement with computational kinetics study of Woon predicting rate coefficients of 3.35 – 3.50 × 10^{-10} cm^3 molecule^{-1} s^{-1} over the 100 – 300K temperature range.[113] This implies that reaction efficiencies are close to unity and that the reaction pathways have no significant energetic barrier. For CN + toluene the measured rate coefficient is 1.3 × 10^{-10} cm^3 molecule^{-1} s^{-1} at 105 K with biexponential profiles reported at higher temperatures although no satisfying explanation is given for the latter observation.[112]

Synchrotron product detection studies of the CN radical with benzene and toluene have also been reported.[112] In these room temperature studies the detected products are consistent with addition then H loss processes (Scheme 6). The CN + benzene reaction gives rise to a clear cyanobenzene (*m/z* 103)

product with no reported detection of isocyano benzene, which is predicted to have a lower vertical ionization energy (VIE of 9.5 eV[112]) than its –CN counterpart. There is no evidence of phenyl radical (C_5H_6) formation that would arise from direct H-abstraction and HCN formation. A CN + benzene CMB study has been performed at collision energies of 19.5 kcal mol^{-1} (81.6 kJ mol^{-1}) and 34.4 kcal mol^{-1} (143.9 kJ mol^{-1}) and reports one product channel, C_6H_5CN + H, with a reaction exothermicity of 80-95 kJ mol^{-1} in good agreement with computational predictions of 95 kJ mol^{-1}.[114] This study also reports that the reaction products are formed from an intermediate that decomposes with a lifetime longer than a rotation period. These findings are in agreement with the aforementioned synchrotron photoionization study on this reaction. The CMB study also reports calculations for the C_6H_5-NC + H product channel – the isocyano analogue – residing -4.9 kJ mol^{-1} below the energy of the reactants but with a +29.5 kJ mol^{-1} transition state barrier along the pathway to this product channel. Hence, this channel is not likely to compete at moderate to low temperatures and collision energies.

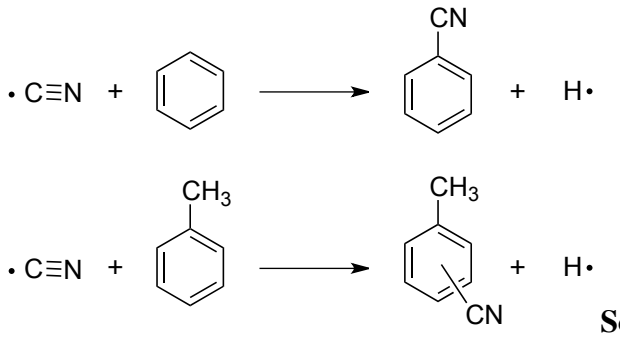

Scheme 6

For CN + toluene, the one detected product is also a CN addition and H elimination product at *m/z* 117 but in this case there is the possibility of different cyanotoluene isomers. The *ortho*, *meta* and *para* isomers have ionization energies that are too similar to distinguish them by the technique. There were no detectable traces of a benzyl + HCN channel nor a cyanobenzene + CH_3 channel. There are currently no other reported kinetic studies for the room temperature CN + toluene reaction and there is scope for further systematic kinetic and product studies on this reaction.

Extending on these CN radical reactions with benzene and toluene, Landera and Mebel have reported computational studies of CN (and C_2H) reactions with styrene ($C_6H_5CH=CH_2$) and N-methylenebenzenamine (C_6H_5-N=CH_2) with an eye on the formation pathways leading to azanaphthalenes via consecutive CN (and/or C_2H) additions.[115] Due to entrance channels that are free from significant thermodynamic barriers, and that H loss is a common pathways of activated intermediates, building up large molecular-weight species including bicyclics is feasible under low temperature conditions and low pressures. Notably, formation of the second ring is initiated by radical addition at the *ortho* position. As an example, CN addition to styrene at the *ortho* carbon leads to formation of 2-vinybenzonitrile, then C_2H addition to the *ortho* carbon of 2-vinylbenzonitrile leads to 1-ethynyl-2-azanaphthalene.[115] More complex combinations of CN and C_2H addition reactions are also reported.[116]

The understanding of molecular weight growth chemistry and feasible ring-formation pathways is vital for the establishment of models and mechanisms that reproduce the formation of particles at both low temperatures, for example organic particles on Titan where temperatures are around 100 K, and soot formation in high-temperature combustion environments. These proposed CN mechanisms are yet to be verified experimentally and, as pointed out by Landera and Mebel in the aforementioned studies, VUV photoionization mass spectrometry experiments should, in principle, be well suited to these reactions since photoionization onsets and photoionization spectra can be used to signify the detection of particular isomers. Photolysis methods for generating CN, (e.g. ICN + 266 nm) can be complicated by significant photodissociation of the co-reactant especially in larger aromatic species.

4. Conclusion and perspective

In this Perspective we have outlined advancements in understanding the mechanisms for reactions of hydrocarbons with CH and CN radicals focusing on isomer-resolved product detection techniques, kinetics measurement over a wide range of temperature, and theoretical calculations. We hope that it hasn't escaped the reader's attention that for seemingly simple reaction pairs, the details that affect

product branching ratios can be complex and sometimes difficult to predict. Furthermore, accurate and comprehensive detection of reaction products, with isomer differentiation, is often non-trivial. It is apparent that a more complete understanding of reaction dynamics is afforded when a suite of experimental and theoretical techniques are used in combination.

The success of photoionization mass spectrometry based methods has revitalized activities around disentangling product isomer in gas-phase reaction environments. Currently, it remains that these methods still require reference absolute photoionization cross sections for accurate quantitative information. This can be a limitation especially for reaction products that are not easy to isolate for the attainment of pure reference spectra. One can imagine in the future that VUV tabletop light sources that rival today's synchrotron VUV sources will become available, thus expanding the libraries of reference spectra and allowing for the characterization of more complex and transient molecules. Expanding the conditions (pressure and temperature) of experimental data sets is also still needed. It is possible that more sophisticated mass spectrometry strategies, such as those developed for proteomics where molecular fragmentation patterns are mined to identify molecular structure, might also be implemented as larger molecular weight species are experimentally tackled.

Computational techniques that allow for accurate prediction of absolute photoionization cross-sections for common hydrocarbon gas-phase products are not generally available and such predictions would be very valuable, particularly for exotic and transient species. Also, the understanding of entrance channel pathways for radical + neutral reactions is rather incomplete and this becomes especially pertinent to reactions where numerous radical addition sites are possible. If different adduct sites lead to distinct product isomers, then product detections coupled with computational insights will provide important insight into this area. Finally, the exciting developments of synchrotron and laboratory-based experiments for probing product isomers continues to reveal mechanisms and fundamental processes of radical + neutral reactions while enlightening our understanding of reactive gas-phase environments.

ACKNOWLEDGMENTS

The authors are eternally grateful to the past and present colleagues, collaborators and mentors of the ALS Kinetics Team, particularly D. L. Osborn, J. D. Savee, O. Weltz, T. M. Selby, S. Soorkia, H. Johanson, C. A. Taatjes and S. R. Leone. They are also sincerely grateful for the support of LBNL ALS Chemical Dynamics beamline including M. Ahmed and K. R. Wilson, B. B. Kirk and D. Taube. Kirk and Savee are also acknowledged for their wise advice and thoughts on this manuscript. Trevitt acknowledges funding support from the Australian Research Council (DP1094135, DP130100862) and some travel support funding from the Australian Synchrotron's ISAP program. Goulay acknowledges support form West Virginia University.

References

[1] M. Muto, H. Watanabe, R. Kurose, S. Komori, S. Balusamy, S. Hochgreb, *Fuel* **2015**, *142*, 152-163.

[2] D. Shimokuri, S. Fukuba, S. Ishizuka, *Proc. Combust. Inst.* **2015**, *35*, 3573-3580.

[3] B. Sundaram, A. Y. Klimenko, M. J. Cleary, *Proc. Combust. Inst.* **2015**, *35*, 1517-1525.

[4] B. M. Jones, F. T. Zhang, R. I. Kaiser, A. Jamal, A. M. Mebel, M. A. Cordiner, S. B. Charnley, *Proc. Natl. Acad. Sci. U. S. A.* **2011**, *108*, 452-457.

[5] S. Lebonnois, *Planet. Space Sci.* **2005**, *53*, 486-497.

[6] V. A. Krasnopolsky, *Icarus* **2009**, *201*, 226-256.

[7] P. P. Lavvas, A. Coustenis, I. M. Vardavas, *Planet. Space Sci.* **2008**, *56*, 27-66.

[8] M. E. Monge, T. Rosenorn, O. Favez, M. Mueller, G. Adler, A. A. Riziq, Y. Rudich, H. Herrmann, C. George, B. D'Anna, *Proc. Natl. Acad. Sci. U. S. A.* **2012**, *109*, 6840-6844.

[9] V. Perraud, E. A. Bruns, M. J. Ezell, S. N. Johnson, Y. Yu, M. L. Alexander, A. Zelenyuk, D. Imre, W. L. Chang, D. Dabdub, et al., *Proc. Natl. Acad. Sci. U. S. A.* **2012**, *109*, 2836-2841.

[10] A. Coustenis, G. Bampasidis, R. K. Achterberg, P. Lavvas, D. E. Jennings, C. A. Nixon, N. A. Teanby, S. Vinatier, F. M. Flasar, R. C. Carlson, et al., *Astrophys. J* **2013**, *779*, 177.

[11] D. Cordier, O. Mousis, J. I. Lunine, S. Lebonnois, P. Rannou, P. Lavvas, L. Q. Lobo, A. G. M. Ferreira, *Planet. Space Sci.* **2012**, *61*, 99-107.

[12] M. Kohler, A. Brockhinke, M. Braun-Unkhoff, K. Kohse-Hoïnghaus, *J. Phys. Chem. A* **2010**, *114*, 4719-4734.

[13] K. J. Rensberger, J. B. Jeffries, R. A. Copeland, K. Kohse-Höinghaus, M. L. Wise, D. R. Crosley, *Appl. Opt.* **1989**, *28*, 3556-3566.

[14] A. Canosa, I. R. Sims, D. Travers, I. W. M. Smith, B. R. Rowe, *Astron. Astrophys.* **1997**, *323*, 644-651.

[15] S. B. Morales, C. J. Bennett, S. D. Le Picard, A. Canosa, I. R. Sims, B. J. Sun, P. H. Chen, A. H. H. Chang, V. V. Kislov, A. M. Mebel, *Astrophys. J* **2011**, *742*, 26.

[16] S. B. Morales, S. D. Le Picard, A. Canosa, I. R. Sims, *Faraday Discuss.* **2010**, *147*, 155-171.

[17] A. Gardez, G. Saidani, L. Biennier, R. Georges, E. Hugo, V. Chandrasekaran, V. Roussel, B. Rowe, K. P. J. Reddy, E. Arunan, *Int. J. Chem. Kinet.* **2012**, *44*, 753-766.

[18] G. Saidani, Y. Kalugina, A. Gardez, L. Biennier, R. Georges, F. Lique, *J. Chem. Phys.* **2013**, *138*, 124308.

[19] J. V. Michael, K. P. Lim, *Ann. Rev. Phys. Chem.* **1993**, *44*, 429-458.

[20] R. S. Tranter, P. T. Lynch, *Rev. Sci. Instrum.* **2013**, *84*,

[21] M. A. Blitz, P. W. Seakins, *Chem. Soc. Rev.* **2012**, *41*, 6318-6347.

[22] R. I. Kaiser, *Chem. Rev.* **2002**, *102*, 1309-1358.

[23] P. Casavecchia, N. Balucani, L. Cartechini, G. Capozza, A. Bergeat, G. G. Volpi, *Faraday Discuss.* **2001**, *119*, 27-49.

[24] M. Teresa Baeza-Romero, M. A. Blitz, A. Goddard, P. W. Seakins, *Int. J. Chem. Kinet.* **2012**, *44*, 532-545.

[25] D. L. Osborn, P. Zou, H. Johnsen, C. C. Hayden, C. A. Taatjes, V. D. Knyazev, S. W. North, D. S. Peterka, M. Ahmed, S. R. Leone, *Rev. Sci. Instrum.* **2008**, *79*, 104103.

[26] C. A. Taatjes, N. Hansen, D. L. Osborn, K. Kohse-Hoeinghaus, T. A. Cool, P. R. Westmoreland, *Phys. Chem. Chem. Phys.* **2008**, *10*, 20-34.

[27] R. I. Kaiser, X. Gu, F. Zhang, P. Maksyutenko, *Phys. Chem. Chem. Phys.* **2012**, *14*, 575-588.

[28] F. Zhang, P. Maksyutenko, R. I. Kaiser, *Phys. Chem. Chem. Phys.* **2012**, *14*, 529-537.

[29] P. Maksyutenko, F. Zhang, X. Gu, R. I. Kaiser, *Phys. Chem. Chem. Phys.* **2011**, *13*, 240-252.

[30] X. Gu, F. Zhang, R. I. Kaiser, *J. Phys. Chem. A* **2008**, *112*, 9607-9613.

[31] N. Balucani, O. Asvany, A. H. H. Chang, S. H. Lin, Y. T. Lee, R. I. Kaiser, Y. Osamura, *J. Chem. Phys.* **2000**, *113*, 8643.

[32] P. Casavecchia, F. Leonori, N. Balucani, R. Petrucci, G. Capozza, E. Segoloni, *Phys. Chem. Chem. Phys.* **2009**, *11*, 46-65.

[33] C. Naulin, N. Daugey, K. M. Hickson, M. Costes, *J. Phys. Chem. A* **2009**, *113*, 14447-14457.

[34] J.-C. Loison, J. Daranlot, A. Bergeat, F. Caralp, R. Mereau, K. M. Hickson, *J. Phys. Chem. A* **2010**, *114*, 13326-13336.

[35] P. Rupper, F. Merkt, *Rev. Sci. Instrum.* **2004**, *75*, 613-622.

[36] C. C. Wang, Y. T. Lee, J. J. Lin, J. Shu, Y. Y. Lee, X. M. Yang, *J. Chem. Phys.* **2002**, *117*, 153-160.

[37] S.-H. Lee, C.-H. Chin, W.-K. Chen, W.-J. Huang, C.-C. Hsieh, *Phys. Chem. Chem. Phys.* **2011**, *13*, 8515-8525.

[38] C.-H. Chin, W.-K. Chen, W.-J. Huang, Y.-C. Lin, S.-H. Lee, *Icarus* **2013**, *222*, 254-262.

[39] A. Bodi, P. Hemberger, T. Gerber, B. Sztaray, *Rev. Sci. Instrum.* **2012**, *83*, 083105.

[40] S. R. Leone, M. Ahmed, K. R. Wilson, *Phys. Chem. Chem. Phys.* **2010**, *12*, 6564-6578.

[41] G. A. Garcia, B. K. Cunha de Miranda, M. Tia, S. Daly, L. Nahon, *Rev. Sci. Instrum.* **2013**, *84*, 053112.

[42] J. Kruger, G. A. Garcia, D. Felsmann, K. Moshammer, A. Lackner, A. Brockhinke, L. Nahon, K. Kohse-Hoinghaus, *Phys. Chem. Chem. Phys.* **2014**, *16*, 22791-22804.

[43] P. Osswald, P. Hemberger, T. Bierkandt, E. Akyildiz, M. Kohler, A. Bodi, T. Gerber, T. Kasper, *Rev. Sci. Instrum.* **2014**, *85*, 025101.

[44] F. Goulay, A. J. Trevitt, G. Meloni, T. M. Selby, D. L. Osborn, C. A. Taatjes, L. Vereecken, S. R. Leone, *J. Am. Chem. Soc.* **2009**, *131*, 993-1005.

[45] A. Bodi, P. Hemberger, D. L. Osborn, B. Sztaray, *J. Phys. Chem. Lett.* **2013**, *4*, 2948-2952.

[46] P. Hemberger, A. J. Trevitt, T. Gerber, E. Ross, G. da Silva, *J. Phys. Chem. A* **2014**, *118*, 3593-3604.

[47] L. Yan, F. Cudry, W. Li, A. G. Suits, *J. Phys. Chem. A* **2013**, *117*, 11890-11895.

[48] F. Cudry, J. M. Oldham, S. Lingenfelter, A. G. Suits, *J. Phys. Chem. A* **2015**, *119,* 460–467

[49] K. Prozument, G. B. Park, R. G. Shaver, A. K. Vasiliou, J. M. Oldham, D. E. David, J. S. Muenter, J. F. Stanton, A. G. Suits, G. B. Ellison, et al., *Phys. Chem. Chem. Phys.* **2014**, *16*, 15739-15751.

[50] C. Abeysekera, L. N. Zack, G. B. Park, B. Joalland, J. M. Oldham, K. Prozument, N. M. Ariyasingha, I. R. Sims, R. W. Field, A. G. Suits, *J. Chem. Phys.* **2014**, *141*, 214203

[51] J. M. Oldham, C. Abeysekera, B. Joalland, L. N. Zack, K. Prozument, I. R. Sims, G. B. Park, R. W. Field, A. G. Suits, *J. Chem. Phys.* **2014**, *141*, 154202

[52] M. Gerin, M. De Luca, J. R. Goicoechea, E. Herbst, E. Falgarone, B. Godard, T. A. Bell, A. Coutens, M. Kazmierczak, P. Sonnentrucker, et al., *Astron. Astrophys.* **2010**, *521*, L16

[53] N. Love, R. N. Parthasarathy, S. R. Gollahalli, *Int. J. Green Energy* **2011**, *8*, 113-120.

[54] F. V. Tinaut, M. Reyes, B. Gimenez, J. V. Pastor, *Energy & Fuels* **2011**, *25*, 119-129.

[55] J. Zhou, E. R. Fisher, *J. Phys. Chem. B* **2006**, *110*, 21911-21919.

[56] N. Galland, F. Caralp, Y. Hannachi, A. Bergeat, J. C. Loison, *J. Phys. Chem. A* **2003**, *107*, 5419-5426.

[57] P. Fleurat-Lessard, J. C. Rayez, A. Bergeat, J. C. Loison, *Chem. Phys.* **2002**, *279*, 87-99.

[58] J.-C. Loison, A. Bergeat, *Phys. Chem. Chem. Phys.* **2009**, *11*, 655-664.

[59] N. Daugey, P. Caubet, B. Retail, M. Costes, A. Bergeat, G. Dorthe, *Phys. Chem. Chem. Phys.* **2005**, *7*, 2921-2927.

[60] R. A. Brownsword, L. B. Herbert, I. W. M. Smith, D. W. A. Stewart, *J . Chem. Soc., Faraday Trans.* **1996**, *92*, 1087-1094.

[61] P. Bocherel, L. B. Herbert, B. R. Rowe, I. R. Sims, I. W. M. Smith, D. Travers, *J. Phys. Chem.* **1996**, *100*, 3063-3069.

[62] S. D. Le Picard, A. Canosa, B. R. Rowe, R. A. Brownsword, I. W. M. Smith, *J. Chem. Soc., Faraday Trans.* **1998**, *94*, 2889-2893.

[63] V. Vasudevan, R. K. Hanson, C. T. Bowman, D. M. Golden, D. F. Davidson, *J. Phys. Chem. A* **2007**, *111*, 11818-11830.

[64] J. A. Miller, C. T. Bowman, *Prog. Energy Combust. Sci.* **1989**, *15*, 287-338.

[65] A. J. Trevitt, M. B. Prendergast, F. Goulay, J. D. Savee, D. L. Osborn, C. A. Taatjes, S. R. Leone, *J. Phys. Chem. A* **2013**, *117*, 6450-6457.

[66] M. A. Blitz, D. Talbi, P. W. Seakins, I. W. M. Smith, *J. Phys. Chem. A* **2012**, *116*, 5877-5885.

[67] F. Goulay, C. Rebrion-Rowe, L. Biennier, S. D. Le Picard, A. Canosa, B. R. Rowe, *J. Phys. Chem. A* **2006**, *110*, 3132-3137.

[68] C. Romanzin, S. Boye-Peronne, D. Gauyacq, Y. Benilan, M. C. Gazeau, S. Douin, *J. Chem. Phys.* **2006**, *125*, 114312.

[69] A. Bergeat, T. Calvo, N. Daugey, J. C. Loison, *J. Phys. Chem. A* **1998**, *102*, 8124-8130.

[70] L. B. Herbert, I. R. Sims, I. Smith, *J. Phys. Chem.* **1996**, *100*, 14928-14935.

[71] F. Goulay, A. Derakhshan, E. Maher, A. J. Trevitt, J. D. Savee, A. M. Scheer, D. L. Osborn, C. A. Taatjes, *Phys. Chem. Chem. Phys.* **2013**, *15*, 4049-4058.

[72] J. Marcelo Ribeiro, A. M. Mebel, *J. Phys. Chem. A* **2014**, *118*, 9080-9086.

[73] K. McKee, M. A. Blitz, K. J. Hughes, M. J. Pilling, H. B. Qian, A. Taylor, P. W. Seakins, *J. Phys. Chem. A* **2003**, *107*, 5710-5716.

[74] T. L. Nguyen, A. M. Mebel, S. H. Lin, R. I. Kaiser, *J. Phys. Chem. A* **2001**, *105*, 11549-11559.

[75] D. Polino, S. J. Klippenstein, L. B. Harding, Y. Georgievskii, *J. Phys. Chem. A* **2013**, *117*, 12677-12692.

[76] W. Boullart, W. Devriendt, R. Borms, J. Peeters, *J. Phys. Chem.* **1996**, *100*, 998-1007.

[77] L. R. McCunn, B. L. FitzPatrick, M. J. Krisch, L. J. Butler, C. W. Liang, J. J. Lin, *J. Chem. Phys.* **2006**, *125*, 133306

[78] H. M. T. Nguyen, H. T. Nguyen, T.-N. Nguyen, H. Van Hoang, L. Vereecken, *J. Phys. Chem. A* **2014**, *118*, 8861-8871

[79] Y. Li, H.-l. Liu, Z.-J. Zhou, X.-R. Huang, C.-C. Sun, *J. Phys. Chem. A* **2010**, *114*, 9496-9506.

[80] S. Soorkia, C. A. Taatjes, D. L. Osborn, T. M. Selby, A. J. Trevitt, K. R. Wilson, S. R. Leone, *Phys. Chem. Chem. Phys.* **2010**, *12*, 8750-8758.

[81] R. Hoffmann, D. M. Hayes, P. S. Skell, *J. Phys. Chem.* **1972**, *76*, 664-669.

[82] R. C. Dobson, D. M. Hayes, R. Hoffmann, *J. Am. Chem. Soc.* **1971**, *93*, 6188-6192.

[83] R. Hoffmann, *J. Am. Chem. Soc.* **1968**, *90*, 1475-1485.

[84] A. Rauk: Orbital Interaction Theory of Organic Chemistry, Wiley, 2001.

[85] B. Zurawski, W. Kutzelnigg, *J. Am. Chem. Soc.* **1978**, *100*, 2654-2659.

[86] T. H. Dunning, L. B. Harding, R. A. Bair, R. A. Eades, R. L. Shepard, *J. Phys. Chem.* **1986**, *90*, 344-356.

[87] T. H. Lowry, K. Schueller Richardson: Mechanism and theory in organic chemistry, Harper & Row, New York, NY, 1987.

[88] H. Thiesemann, J. MacNamara, C. A. Taatjes, *J. Phys. Chem. A* **1997**, *101*, 1881-1886.

[89] F. Goulay, A. J. Trevitt, J. D. Savee, J. Bouwman, D. L. Osborn, C. A. Taatjes, K. R. Wilson, S. R. Leone, *J. Phys. Chem. A* **2012**, *116*, 6091-6106.

[90] J. Berkowitz, G. B. Ellison, D. Gutman, *J. Phys. Chem.* **1994**, *98*, 2744-2765.

[91] J. F. Lockyear, M. Fournier, I. R. Sims, J.-C. Guillemin, C. A. Taatjes, D. L. Osborn, S. R. Leone, *Int. J. Mass Spectrom.* **2015**, *378*, 232-245.

[92] S. Pakhira, B. S. Lengeling, O. Olatunji-Ojo, M. Caffarel, M. Frenklach, W. A. Lester, *J. Phys. Chem. A* **2015**, *119* ,4214-4223

[93] V. A. Krasnopolsky, *Icarus* **2014**, *236*, 83-91.

[94] J. A. Sebree, M. G. Trainer, M. J. Loeffler, C. M. Anderson, *Icarus* **2014**, *236*, 146-152.

[95] M. L. Cable, S. M. Hörst, C. He, A. M. Stockton, M. F. Mora, M. A. Tolbert, M. A. Smith, P. A. Willis, *Earth Planet. Sci. Lett.* **2014**, *403*, 99-107.

[96] K. L. Gannon, D. R. Glowacki, M. A. Blitz, K. J. Hughes, M. J. Pilling, P. W. Seakins, *J. Phys. Chem. A* **2007**, *111*, 6679-6692.

[97] A. Singh, Shivani, A. Misra, P. Tandon, *Res. Astron. Astrophys.* **2014**, *14*, 275-284.

[98] R. Bachiller, A. Fuente, V. Bujarrabal, F. Colomer, C. Loup, A. Omont, T. De Jong, *Astron. Astrophys.* **1997**, *319*, 235-243.

[99] K. Kohse-Hoinghaus, P. Oßwald, T. A. Cool, T. Kasper, N. Hansen, F. Qi, C. K. Westbrook, P. R. Westmoreland, *Angew. Chem. Int. Ed.* **2010**, *49*, 3572-3597.

[100] I. W. M. Smith, *Angew. Chem. Int. Ed. Engl.* **2006**, *45*, 2842-2861.

[101] N. Choi, M. A. Blitz, K. McKee, M. J. Pilling, P. W. Seakins, *Chem. Phys. Lett.* **2004**, *384*, 68-72.

[102] L. Vereecken, P. D. Groof, J. Peeters, *Phys. Chem. Chem. Phys.* **2003**, *5*, 5070.

[103] F. Leonori, R. Petrucci, X. Wang, P. Casavecchia, N. Balucani, *Chem. Phys. Lett.* **2012**, *553*, 1-5.

[104] A. J. Trevitt, F. Goulay, G. Meloni, D. L. Osborn, C. A. Taatjes, S. R. Leone, *Int. J. Mass Spectrom.* **2009**, *280*, 113-118.

[105] NIST, Standard Reference Database Number 69, NIST Chemistry WebBook, National Institute of Standards and Technology, Gaithersburg MD, 20899 (http://webbook.nist.gov). 2005.

[106] R. I. Kaiser, N. Balucani, *Acc. Chem. Res.* **2001**, *34*, 699-706.

[107] D. S. N. Parker, A. M. Mebel, R. I. Kaiser, *Chem. Soc. Rev.* **2014**, *43*, 2701-2713.

[108] C. H. Huang, R. I. Kaiser, A. H. H. Chang, *J. Phys. Chem. A* **2009**, *113*, 12675-12685.

[109] A. J. Trevitt, S. Soorkia, J. D. Savee, T. S. Selby, D. L. Osborn, C. A. Taatjes, S. R. Leone, *J. Phys. Chem. A* **2011**, *115*, 13467-13473.

[110] A. D. Estillore, L. M. Visger, R. I. Kaiser, A. G. Suits, *J. Phys. Chem. Lett.* **2010**, *1*, 2417-2421.

[111] A. Jamal, A. M. Mebel, *J. Phys. Chem. A* **2013**, *117*, 741-755.

[112] A. J. Trevitt, F. Goulay, C. A. Taatjes, D. L. Osborn, S. R. Leone, *J. Phys. Chem. A* **2010**, *114*, 1749-1755.

[113] D. E. Woon, *Chem. Phys.* **2006**, *331*, 67-76.

[114] N. Balucani, O. Asvany, A. H. H. Chang, S. H. Lin, Y. T. Lee, R. I. Kaiser, H. F. Bettinger, P. V. Schleyer, H. F. Schaefer, *J. Chem. Phys.* **1999**, *111*, 7457-7471.

[115] A. Landera, A. M. Mebel, *J. Am. Chem. Soc.* **2013**, *135*, 7251-7263.

[116] A. Landera, A. M. Mebel, *Faraday Discuss.* **2010**, *147*, 479-494.